Micro and Nano Systems Letters

LETTER

Open Access

Ethanol-sensing properties of cobalt porphyrin-functionalized titanium dioxide nanoparticles as chemiresistive materials that are integrated into a low power microheater

Kwanhun Kim†, Yunsung Kang†, Kyubin Bae and Jongbaeg Kim*

Abstract

Gaseous ethanol detection has attracted significant interest owing to its practical applications such as in breath analysis, chemical process monitoring, and safety evaluations of food packaging. In this study, titanium dioxide (TiO_2) nanoparticles functionalized with cobalt porphyrin (CoPP) are utilized as resistive ethanol-sensing materials, and are integrated with a suspended micro-heater for low power consumption. The micro-heater with the suspended structure inhibits substrate heat transfer, resulting in power consumption as low as 18 mW when the operating temperature is approximately 300 °C. CoPP functionalization allows an enhanced response (197.8%) to 10 ppm ethanol compared to that of pristine TiO_2 nanoparticles. It is confirmed that the sensor response is reliable upon exposure to 10 ppm ethanol for three cycles. In addition, responses of different magnitude are obtained under exposure to ethanol at various concentrations from 9 to 1 ppm, indicating that the resistance change originates from a charge transfer between the sensing materials and target gas. The sensing mechanism of CoPP-functionalized TiO_2 in relation to charge transfer is analyzed, and the performance of the proposed sensor with previously reported TiO_2-based ethanol sensors is compared. Considering that it is processed by batch fabrication, consumes low power, and offers high sensitivity, the proposed sensor is promising for use as a portable sensor in the distributed monitoring of gaseous ethanol.

Keywords: Ethanol sensor, Titanium dioxide, Cobalt porphyrin, Functionalization, High sensitivity, Low power consumption, Batch fabrication, Gas sensor

Introduction

With the emergence of the Internet of Things and advancements in machine learning, there is significant interest in the collection and processing of physical/chemical information using various sensors at multiple locations. The sensors must be portable so that vast amounts of data can be obtained from various locations. In addition, portable sensors must possess several features, including a small size for module integration, fast response/recovery speed to physical/chemical stimuli, productivity and cost-efficiency, low power consumption, and durability for long-term operation.

Among the goals of using distributed sensor networks is monitoring harmful molecules in the gaseous state; to this end, many researchers have focused on gas sensors for decades. Among the many sensors used to detect harmful gas species, those for the detection of ethanol have received significant attention owing to their practical applications, such as in the breath analysis of

*Correspondence: kimjb@yonsei.ac.kr
†Kwanhun Kim and Yunsung Kang contributed equally to this work
School of Mechanical Engineering, Yonsei University, 50 Yonsei-ro, Seodaemun-gu, Seoul 03722, Republic of Korea

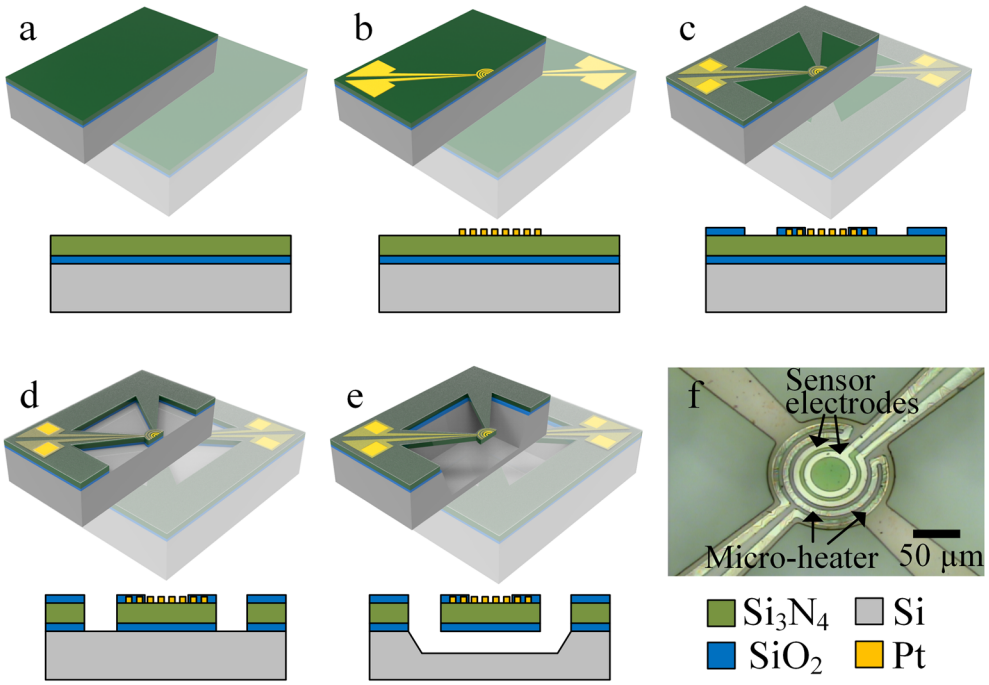

Fig. 1 Fabrication of the sensor platform with the suspended micro-heater. **a** Deposition of 500 nm-thick silicon nitride (Si_3N_4) on a 300 nm-thick silicon dioxide (SiO_2) substrate through low-pressure chemical vapor deposition (CVD). **b** Deposition of a 25/250 nm-thick Ti/Pt film and patterning with photolithography and reactive ion etching (RIE) on the Si_3N_4/SiO_2 substrate. **c** Deposition of a 200 nm-thick SiO_2 film via plasma-enhanced CVD and patterning with photolithography and RIE, leading to the formation of a passivation layer for the heating element. **d** Photolithography and RIE to etch $SiO_2/Si_3N_4/SiO_2$ layers for opening the bare Si layer. **e** Wet etching of the Si substrate using tetramethylammonium hydroxide to form the suspended structure. **f** Optical image of the fabricated sensor platform with the micro-heater

intoxicated drivers [1], chemical process monitoring [2], and safety evaluations of food packaging [3]. Various mechanisms have been proposed to detect gaseous ethanol, such as those that are based on chemiresistive [4], electrochemical [5], and colorimetric sensing [6]. Among them, chemiresistive sensors, which use metal oxide-based materials as ethanol-sensing elements, typically offer advantages such as high sensitivity, cost-effectiveness, and a simple electronic setup for measurement [7, 8]. In general, metal oxide-based sensors require high-temperature operation above 200 °C to efficiently induce a redox reaction of the target gas on the material's surface. The use of titanium dioxide (TiO_2) between various metal oxides has received remarkable attention for gas detection owing to its stability and reliability at high temperatures [9, 10]. Several ethanol sensors that utilize the properties of TiO_2 have also been reported [2, 10–25]. However, except for a few studies, it has largely been challenging to achieve the highly sensitive detection (in several ppm) of ethanol [2, 23–25]. Moreover, most aforementioned studies merely presented the ethanol-sensing characteristics of TiO_2-based materials without considering their productivity and low-power consumption [26, 27], which are required for portable sensors. In our previous work, we presented a batch-producible benzene, toluene, and xylene sensor using TiO_2 nanoparticles functionalized with cobalt porphyrin (CoPP) as sensing materials [28].

This study presents an ethanol sensor using TiO_2 nanoparticles functionalized with CoPP as sensing materials. We also integrated the sensing materials with a suspended micro-heater, enabling the desired heat generation with low power consumption. CoPP functionalization on TiO_2 nanoparticles allowed an increased sensitivity (197.8%) to 10 ppm ethanol compared to pristine nanoparticles. We also investigated the ethanol-sensing characteristics of TiO_2 nanoparticles functionalized with CoPP based on the operating temperatures. The fabricated sensor showed a reliable response under repeated exposure to 10 ppm ethanol. The sensor responses to ethanol at various concentrations are presented in the paper, along with the suggested sensing mechanisms.

Methods and materials

Figure 1 depicts the fabrication process of the sensor platform with the suspended micro-heater. First, 500 nm-thick silicon nitride (Si_3N_4) was deposited on a 300 nm-thick silicon dioxide (SiO_2) substrate through

low-pressure chemical vapor deposition (CVD) (Fig. 1a) to induce low residual stress of a membrane. Subsequently, a 25/250 nm-thick Ti/Pt film was deposited on the Si_3N_4/SiO_2 substrate and patterned via photolithography and reactive ion etching (RIE) to obtain the metal heating element and sensor electrodes in the desired shape (Fig. 1b). A 200 nm-thick SiO_2 film was then deposited via plasma-enhanced CVD and patterned by photolithography and RIE, resulting in the formation of a passivation layer for the heating element (Fig. 1c). Photolithography and RIE were performed to etch the $SiO_2/Si_3N_4/SiO_2$ layers for opening the bare Si layer (Fig. 1d). The opened Si substrate was then wet-etched using tetramethylammonium hydroxide (TMAH) to form the suspended structure (Fig. 1e). We could not observe a fracture of the membrane of the sensor platform when etched in TMAH solution. This would be due to the tri-layered structure ($SiO_2/Si_3N_4/SiO_2$) of membrane, contributing the reduction of residual stress in the membrane with partial compensation of the compressive and tensile stress of the oxide and the nitride, respectively. An optical image of the fabricated sensor platform, including the micro-heater, is presented in Fig. 1 f. The image confirms the formation of the SiO_2 passivation layer except for the part of sensor electrodes. This prevents the undesired effects to the micro-heater arising from the preparation of the sensing materials.

To prepare the sensing materials, we drop-coated a 3.3–3.7 wt% TiO_2 nanoparticle dispersion (titanium(IV) oxide, Sigma-Aldrich) in DI water using a micropipette. It was uniformly formed at the center circle of the sensor platform. E-beam evaporation of CoPP (5,10,15,20-tetraphenyl-21 H,23 H-porphyrin cobalt(II)) was then performed for functionalizing TiO_2. Consequently, the originally insulated sensor electrodes were connected with the electrical channel of the CoPP-functionalized TiO_2 nanoparticles. The material characterization of the TiO_2 nanoparticles, CoPP, and CoPP-functionalized TiO_2 is described in detail elsewhere [28].

For evaluating the ethanol detection capability of the sensor, we placed it in a quartz tube at room temperature. Mass flow controllers were connected to one end of the quartz tube to control the flow rates of dry air and 10 ppm ethanol gas. The total flow rate was fixed at 500 sccm, and ethanol gas at various concentrations was generated and injected into the quartz tube by adjusting the flow rate of each gas. The current change in the CoPP-functionalized TiO_2 nanoparticles on exposure to various concentrations of ethanol, with a fixed input voltage of 3.5 V to the sensor electrodes, was recorded with a computer-controlled source meter (2400, Keithley). To generate heat for efficiently inducing the redox reaction between ethanol and sensing materials, a voltage (3 V) to the micro-heater was applied with direct current (DC) power supply (E3647A, Agilent).

Results and discussion

Figure 2a shows the sensor responses of the pristine TiO_2 nanoparticles and CoPP-functionalized nanoparticles to 10 ppm ethanol. Here, the sensor response is defined as R_{air}/R_{gas} (R_{gas} and R_{air} denote the resistance measured in ethanol and air environment, respectively), because TiO_2 is an n-type semiconducting material, and ethanol is well-known as a reducing gas that provides electrons to sensing materials. Before CoPP functionalization, a sensor using pristine TiO_2 nanoparticles as the sensing material exhibited a response of 6.41 to 10 ppm ethanol. However, the sensor with CoPP functionalization showed a response of 12.68 upon exposure to 10 ppm ethanol, which is approximately twice as high as that of using pristine nanoparticles. These results indicate that CoPP functionalization on TiO_2 nanoparticles is highly advantageous for achieving enhanced sensitivity to ethanol. This result corresponds well with previous studies, where CoPP was suggested to be an effective functionalization material for enhancing the sensitivity to volatile organic compounds, including diverse nanomaterials such as graphene [29], tin dioxide [30], and zinc oxide [31]. Ethanol is also known as a volatile organic compound, and the detailed sensitivity-enhancing mechanism of CoPP-functionalized TiO_2 to ethanol will be discussed later.

Figure 2b shows the relationship between the input voltage of the micro-heater and the corresponding temperature. The operating temperature was indirectly estimated using a resistance temperature detector (RTD) with the micro-heater. The RTD was fabricated together with the sensor platform using the same process. A resistor of the RTD was designed and fabricated at the location where the sensor electrodes were originally positioned. We measured the resistance of the resistor in a furnace at various temperatures and compared it for various input voltages of the micro-heater. This made it possible to estimate the relationship between the input voltage of the micro-heater and the corresponding temperature. Based on the temperature estimation, we investigated the response of the sensor to 10 ppm ethanol at various operating temperatures. The responses of the sensor were 3.12, 9.56, 10.85, 12.68, and 9.94 on exposure to 10 ppm ethanol when the operating temperatures of the micro-heater were 172.64, 217.08, 263.32, 308.6, and 341.72 °C, respectively (Fig. 2c). The optimal temperature of the sensor using CoPP-functionalized TiO_2 as the sensing material was achieved with a micro-heater input voltage of 3.0 V. Notably, at 3.0 V, we achieved a power consumption as low as 18 mW. However, at 3.4 V, at which point the operating temperature increased,

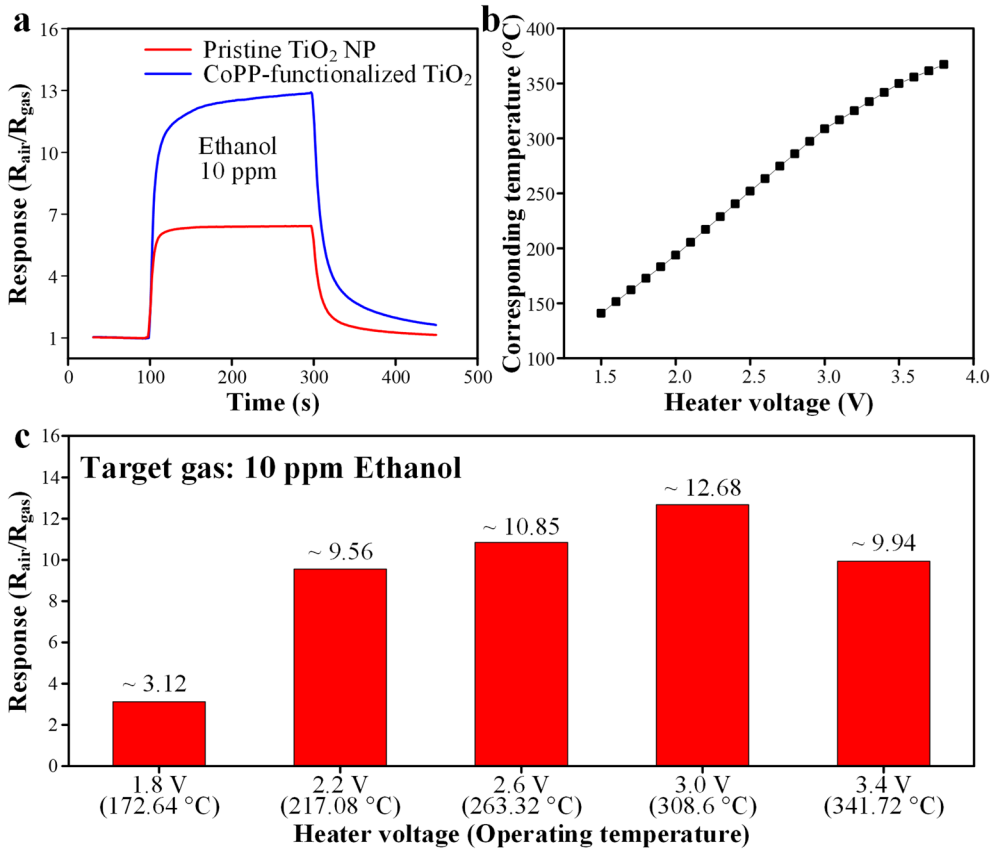

Fig. 2 **a** Sensor response of pristine and CoPP-functionalized TiO_2 nanoparticles to 10 ppm ethanol. **b** Relationship between the input voltage of the micro-heater and corresponding temperature. **c** Sensor response to 10 ppm ethanol at various operating temperatures

the sensor response slightly decreased. This is because the rate of desorption of the reactants exceeded that of absorption of the gas at higher temperatures [32]. Therefore, subsequent characterization using the sensor was performed with a heater input voltage of 3.0 V (i.e., at an operating temperature of 308.6 °C).

Figure 3a depicts the sensor response under repeated exposure to 10 ppm ethanol; there is no remarkable change in the sensor responses. The sensor response to ethanol at various concentrations from 9 down to 1 ppm is presented in Fig. 3b; the sensor response increases as the ethanol concentration increases. These results indicate that the change in the resistance of the sensing materials originated from charge transfer from ethanol gas. The detailed ethanol-sensing mechanism of the CoPP-functionalized TiO_2 nanoparticles was analyzed and is depicted in Fig. 4. Three mechanisms simultaneously occur in ethanol detection using the CoPP-functionalized TiO_2 nanoparticles. The first is a direct interaction between ethanol and CoPP. CoPP itself is known as a gas-sensing material, particularly for volatile organic compounds including ethanol; it also acts as a semiconducting material [33], and reacts with ethanol due to adsorption via π–π interactions and hydrogen bonding [34]. This induces electron transfer from ethanol to CoPP. Subsequently, the transferred electrons migrate from CoPP to TiO_2 due to the difference in the Fermi energy between them [28]. The second is the catalytic reaction between ethanol and oxygen ions near the CoPP and TiO_2 nanoparticles. CoPP is known to act as a catalyst for oxidizing volatile compounds [35]. Hence, the CoPP catalyst enables the oxidization of ethanol, which efficiently induces charge transfer from ethanol to TiO_2. The third mechanism is a redox reaction between ethanol and oxygen ions on TiO_2 nanoparticles without the influence of CoPP, like in other metal oxide-based ethanol sensors. All these mechanisms contribute to a change in the depletion region of the TiO_2 nanoparticles. Thus, an electrical channel composed of TiO_2 nanoparticles is more conductive when exposed to ethanol, enabling the highly sensitive detection of ethanol.

Table 1 compares the sensing performances of the TiO_2-based ethanol sensors. Most previously reported sensors operated at high temperatures with an external

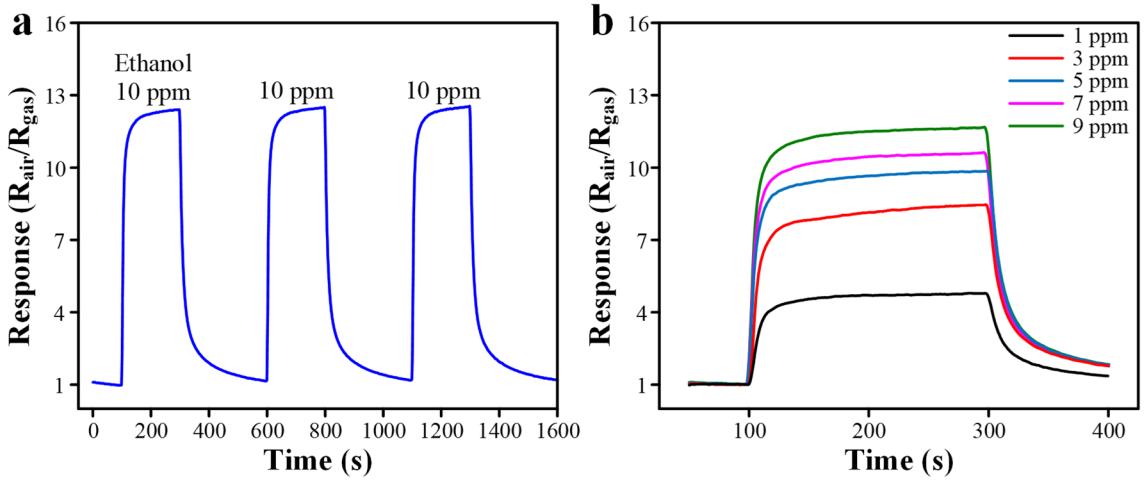

Fig. 3 **a** Sensor response under repeated exposure to 10 ppm ethanol. **b** Sensor response to ethanol at various concentrations from 1 to 9 ppm

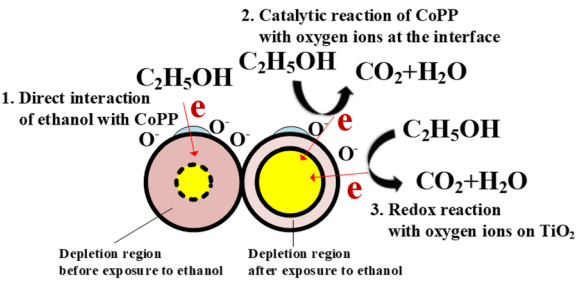

Fig. 4 Detailed ethanol-sensing mechanism of CoPP-functionalized TiO_2 nanoparticles

heating system such as a furnace or a separated hotplate. The operation of such sensors involved extremely high power consumption. Meanwhile, some studies reported TiO_2-based ethanol sensors that could operate at room temperature [2, 17, 19, 21]. However, the TiO_2-based sensing materials exhibited high resistance (on the order of gigaohms) at room temperature, making it difficult to integrate the sensor with simple and inexpensive circuits. By comprehensively considering the sensitivity, power consumption, and limit of detection, our ethanol sensor offers advantages over previously reported sensors.

One aspect of the sensor to be considered is long-term stability. We presented the long-term stability of a sensor with the same sensing materials to toluene [28], and the sensitivity reduced to 60% level after about 5 days. Thus, the long-term stability of the presented sensor to ethanol at a similar level to toluene is expected. Meanwhile, anatase is known as the metastable phase and can easily transform to the most stable rutile phase after heating TiO_2 at temperatures of 450–850 °C [36]. This range is beyond the operating temperatures of our sensor, hence, the decrease in sensitivity after several days might originate from the thermal stability of CoPP. Nevertheless, when considering the sensor can be batch-fabricated at a low cost, the sensors can be easily replaced with another after a certain amount of time. Furthermore, the same sensing materials exhibited a stable long-time operation to toluene for 14 h [28], which means that it can be used with reliability over a certain period of time. Another approach to enhance the thermal stability of CoPP is adding a functional group to increase ionization potential [37]. This can be utilized for enhancing the thermal stability of CoPP.

Conclusions

We demonstrated an ethanol sensor using TiO_2 nanoparticles functionalized with CoPP as sensing materials together with a micro-heater for low power consumption. The sensor platform, including the sensor electrodes and micro-heater on the suspended structure, was batch-fabricated by bulk micromachining. The suspended structure of the micro-heater allowed the power consumption of the sensor to be as low as 18 mW, providing the desired temperatures due to the limited heat transfer through the substrate. We confirmed that CoPP functionalization was effective in achieving high sensitivity to 10 ppm ethanol, allowing a response that was approximately twice higher than that of pristine nanoparticles. Various operating temperatures were achieved with different input voltages of the micro-heater, and the sensor response to 10 ppm ethanol was evaluated at different temperatures. The results indicated that the optimal operating temperature for the CoPP-functionalized TiO_2 nanoparticles to detect ethanol was 308.6 °C. The sensor showed a reliable response under repeated exposure

Table 1 Comparison of the current ethanol-sensing performance with those of previously reported TiO_2-based sensors

Sensing material	Concentration	Response def.	Response	Operating temperature	Power consumption	Limit of detection	Ref.
Ag@TiO_2 nanoparticles	5 ppm	R_a/R_g	4.35	RT	–	0.15 ppm	[2]
Surface-coarsened Ag-TiO_2 nanobelts	500 ppm	R_a/R_g	46.153	200 °C	N/A*	5 ppm	[10]
TiO_2 thin film	100 ppm	$(I_g-I_a)/I_0$	~10	400 °C	N/A*	100 ppm	[11]
TiO_2 nanoparticle	100 ppm	I_g/I_a	~11.5	350 °C	N/A*	20 ppm	[12]
Nb-/Cu-doped TiO_2 nanoparticle	100 ppm	R_a/R_g	~3	400 °C	N/A*	25 ppm	[13]
TiO_2 3D hierarchical nanostructure	100 ppm	R_a/R_g	6.4	350 °C	N/A*	20 ppm	[14]
TiO_2 nanotube	1000 ppm	$(I_g-I_a)/I_a$	13,800	250 °C	N/A*	50 ppm	[15]
Nb-doped TiO_2 nanorods	400 ppm	R_a/R_g	~16	500 °C	N/A*	50 ppm	[16]
TiO_2 nanotube	400 ppm	R_g/R_a	~0.7	RT	–	400 ppm	[17]
TiO_2 nanotube	50 ppm	R_a/R_g	~10	450 °C	26 mW	50 ppm	[18]
TiO_2 nanoparticle thin film	50 ppm	$(R_a-R_g)/R_g\times100$	535%	RT	–	10 ppm	[19]
TiO_2/V_2O_5 branched nanoheterostructures	100 ppm	R_a/R_g	24.6	350 °C	N/A*	20 ppm	[20]
3Dhierarchical flower-like TiO_2microstructures	100 ppm	R_a/R_g	2.25	RT	–	10 ppm	[21]
Anatase@rutile core@shell TiO_2 nanosheets	500 ppm	R_a/R_g	43.9	270 °C	N/A*	50 ppm	[22]
Carbon-doped TiO_2 nanoparticle	1 ppm	$(R_a-R_g)/R_a*100$	34%	150 °C	N/A*	1 ppm	[23]
Ag-loaded TiO_2 nanorod	0.6 ppm	$(I_g-I_a)/I_a$	4.65	200 °C	N/A*	0.6 ppm	[24]
MoS_2/TiO_2 composite	500 ppm	$(R_a-R_g)/R_a\times100$	100%	300 °C	N/A*	1 ppm	[25]
CoPP-functionalized TiO_2 nanoparticles	10 ppm	R_a/R_g	12.68	308.6 °C	18 mW	1 ppm	This work

N/A: not available, *RT:* room temperature

*An external heater, a furnace, or meso-scale heater were used and the exact power consumption of heating element was not specified

to 10 ppm ethanol. The sensor also exhibited an increase in response as the ethanol concentration increased, indicating that the change in resistance originated from the charge transfer between the sensing material and target gas. The mechanism of charge transfer between ethanol and CoPP-functionalized TiO_2 was analyzed. Considering its high sensitivity, low power consumption, cost-effectiveness due to batch fabrication, and small size, our sensor would be promising for portable applications requiring ethanol detection.

Abbreviations

TiO_2: Titanium dioxide; CoPP: Cobalt porphyrin; $Si3N_4$: Silicon nitride; SiO_2: Silicon dioxide; CVD: Chemical vapor deposition; RTD: Resistance temperature detector.

Acknowledgements

Not applicable.

Author contributions

KK, YK, KB and JK developed the idea. KK and YK carried out fabrication, measurement, and analysis of the results, and wrote the manuscript. KB supported fabrication process and measurement. JK supervised the research and reviewed the manuscript. All authors read and approved the final manuscript.

Funding

This work was supported by the National Research Foundation of Korea(NRF) grant funded by the Korea government(MSIT). (No. 2021R1A2B5B03002850)

Availability of data and materials

All data generated or analyzed during this study are included in this published article.

Declarations

Competing interests

The authors declare that they have no competing interests.

Received: 12 December 2021 Accepted: 27 March 2022
Published online: 19 April 2022

References

1. Meng J, Li H, Zhao L, Lu J, Pan C, Zhang Y et al (2020) Triboelectric nanogenerator enhanced schottky nanowire sensor for highly sensitive ethanol detection. Nano Lett 20(7):4968–4974. https://doi.org/10.1021/acs.nanolett.0c01063
2. Zhu Z, Kao C-T, Wu R-J (2014) A highly sensitive ethanol sensor based on Ag@TiO2 nanoparticles at room temperature. Appl Surf Sci 320:348–355. https://doi.org/10.1016/j.apsusc.2014.09.108
3. Haron W, Wisitsoraat A, Wongnawa S (2017) Nanostructured perovskite oxides – LaMO3 (M = Al, Co, Fe) prepared by co-precipitation method and their ethanol-sensing characteristics. Ceram Int 43(6):5032–5040. https://doi.org/10.1016/j.ceramint.2017.01.013
4. Righettoni M, Amann A, Pratsinis SE (2015) Breath analysis by nanostructured metal oxides as chemo-resistive gas sensors. Mater Today 18(3):163–171. https://doi.org/10.1016/j.mattod.2014.08.017
5. Zhang J, Jiang G, Goledzinowski M, Comeau FJE, Li K, Cumberland T et al (2017) Green solid electrolyte with cofunctionalized nanocellulose/graphene oxide interpenetrating network for electrochemical gas sensors. Small Methods 1(11):1700237. https://doi.org/10.1002/smtd.201700237
6. Mustafa F, Carhart M, Andreescu S (2021) A 3D-printed breath analyzer incorporating CeO2 nanoparticles for colorimetric enzyme-based ethanol sensing. ACS Appl Nano Mater 4(9):9361–9369. https://doi.org/10.1021/acsanm.1c01826
7. Sun Y-F, Liu S-B, Meng F-L, Liu J-Y, Jin Z, Kong L-T et al (2012) Metal oxide nanostructures and their gas sensing properties: a review. Sensors. https://doi.org/10.3390/s120302610
8. Dey A (2018) Semiconductor metal oxide gas sensors: a review. Mater Sci Eng B 229:206–217. https://doi.org/10.1016/j.mseb.2017.12.036
9. Moon HG, Shim Y-S, Jang HW, Kim J-S, Choi KJ, Kang C-Y et al (2010) Highly sensitive CO sensors based on cross-linked TiO2 hollow hemispheres. Sens Actuators B 149(1):116–121. https://doi.org/10.1016/j.snb.2010.06.014
10. Hu P, Du G, Zhou W, Cui J, Lin J, Liu H et al (2010) Enhancement of ethanol vapor sensing of TiO2 nanobelts by surface engineering. ACS Appl Mater Interfaces 2(11):3263–3269. https://doi.org/10.1021/am100707h
11. Garzella C, Comini E, Tempesti E, Frigeri C, Sberveglieri G (2000) TiO2 thin films by a novel sol–gel processing for gas sensor applications. Sens Actuators B 68(1):189–196. https://doi.org/10.1016/S0925-4005(00)00428-7
12. Rella R, Spadavecchia J, Manera MG, Capone S, Taurino A, Martino M et al (2007) Acetone and ethanol solid-state gas sensors based on TiO2 nanoparticles thin film deposited by matrix assisted pulsed laser evaporation. Sens Actuators B 127(2):426–431. https://doi.org/10.1016/j.snb.2007.04.048
13. Teleki A, Bjelobrk N, Pratsinis SE (2008) Flame-made Nb- and Cu-doped TiO2 sensors for CO and ethanol. Sens Actuators B 130(1):449–457. doi: https://doi.org/10.1016/j.snb.2007.09.008
14. Wang C, Yin L, Zhang L, Qi Y, Lun N, Liu N (2010) Large scale synthesis and gas-sensing properties of anatase TiO2 three-dimensional hierarchical nanostructures. Langmuir 26(15):12841–12848. https://doi.org/10.1021/la100910u
15. Kwon Y, Kim H, Lee S, Chin I-J, Seong T-Y, Lee WI et al (2012) Enhanced ethanol sensing properties of TiO2 nanotube sensors. Sens Actuators B 173:441–446. https://doi.org/10.1016/j.snb.2012.07.062
16. Singh S, Kaur H, Singh VN, Jain K, Senguttuvan TD (2012) Highly sensitive and pulse-like response toward ethanol of Nb doped TiO2 nanorods based gas sensors. Sens Actuators B 171–172:899–906. doi: https://doi.org/10.1016/j.snb.2012.06.002
17. Perillo PM, Rodríguez DF (2012) The gas sensing properties at room temperature of TiO2 nanotubes by anodization. Sensors Actuators B Chem 171:639. https://doi.org/10.1016/j.snb.2012.05.047
18. Kida T, Seo M-H, Suematsu K, Yuasa M, Kanmura Y, Shimanoe K (2013) A micro gas sensor using TiO2 nanotubes to detect volatile organic compounds. Appl Phys Express 6(4):047201. https://doi.org/10.7567/apex.6.047201
19. Pandeeswari R, Karn RK, Jeyaprakash BG (2014) Ethanol sensing behaviour of sol–gel dip-coated TiO2 thin films. Sens Actuators B 194:470–477. doi: https://doi.org/10.1016/j.snb.2013.12.122
20. Wang Y, Zhou Y, Meng C, Gao Z, Cao X, Li X et al (2016) A high-response ethanol gas sensor based on one-dimensional TiO2/V2O5 branched nanoheterostructures. Nanotechnology 27(42):425503. https://doi.org/10.1088/0957-4484/27/42/425503
21. Wang M, Zhu Y, Meng D, Wang K, Wang C (2020) A novel room temperature ethanol gas sensor based on 3D hierarchical flower-like TiO2 microstructures. Mater Lett 277:128372. doi: https://doi.org/10.1016/j.matlet.2020.128372
22. Zhang J, Chen C, Lu H, Leng D, Li G, Liu Y et al (2020) Construction of anatase@rutile core@shell TiO2 nanosheets with controllable shell layer thicknesses for enhanced ethanol sensing. Sens Actuators B 325:128815. https://doi.org/10.1016/j.snb.2020.128815
23. Raghu AV, Karuppanan KK, Pullithadathil B (2019) Controlled carbon doping in anatase TiO2 (101) facets: superior trace-level ethanol gas sensor performance and adsorption kinetics. Adv Mater Interfaces 6(4):1801714. https://doi.org/10.1002/admi.201801714
24. Kılıç A, Alev O, Özdemir O, Arslan L, Büyükköse S, Öztürk ZZ (2021) The effect of Ag loading on gas sensor properties of TiO2 nanorods. Thin Solid Films 726:138662. https://doi.org/10.1016/j.tsf.2021.138662
25. Singh S, Sharma S (2022) Temperature dependent selective detection of ethanol and methanol using MoS2/TiO2 composite. Sens Actuators B 350:130798. doi: https://doi.org/10.1016/j.snb.2021.130798
26. Jang W, Park J-S, Lee K-W, Roh Y (2018) Methane and hydrogen sensing properties of catalytic combustion type single-chip micro gas sensors with two different Pt film thicknesses for heaters. Micro Nano Syst Lett 6(1):7. https://doi.org/10.1186/s40486-018-0069-y
27. Lee JE, Lim CK, Song H, Choi S-Y, Lee D-S (2021) A highly smart MEMS acetone gas sensors in array for diet-monitoring applications. Micro Nano Syst Lett 9(1):10. https://doi.org/10.1186/s40486-021-00136-1
28. Kang Y, Kim K, Cho B, Kwak Y, Kim J (2020) Highly sensitive detection of benzene, toluene, and xylene based on CoPP-functionalized tio2 nanoparticles with low power consumption. ACS Sens 5(3):754–763. https://doi.org/10.1021/acssensors.9b02310
29. Pyo S, Choi J, Kim J (2019) Improved photo- and chemical-responses of graphene via porphyrin-functionalization for flexible, transparent, and sensitive sensors. Nanotechnology 30(21):215501. doi: https://doi.org/10.1088/1361-6528/ab048d
30. Cho B, Lee K, Pyo S, Kim J (2018) Fabrication and characterization of VOC sensor array based on SnO2 and ZnO nanoparticles functionalized by metalloporphyrins. Micro Nano Syst Lett 6(1):10. https://doi.org/10.1186/s40486-018-0072-3
31. Lee K, Baek D-H, Choi J, Kim J (2018) Suspended CoPP-ZnO nanorods integrated with micro-heaters for highly sensitive VOC detection. Sens Actuators B 264:249–254. doi: https://doi.org/10.1016/j.snb.2018.02.161
32. Bendahan M, Guérin J, Boulmani R, Aguir K (2007) WO3 sensor response according to operating temperature: experiment and modeling. Sens Actuators B 124(1):24–29. https://doi.org/10.1016/j.snb.2006.11.036
33. Paolesse R, Nardis S, Monti D, Stefanelli M, Di Natale C (2017) Porphyrinoids for chemical sensor applications. Chem Rev 117(4):2517–2583. https://doi.org/10.1021/acs.chemrev.6b00361
34. D'Amico A, Di Natale C, Paolesse R, Macagnano A, Mantini A (2000) Metalloporphyrins as basic material for volatile sensitive sensors. Sens Actuators B 65(1):209–215. doi: https://doi.org/10.1016/S0925-4005(99)00342-1
35. Nardis S, Monti D, Natale CD, D'Amico A, Siciliano P, Forleo A et al (2004) Preparation and characterization of cobalt porphyrin modified tin dioxide films for sensor applications. Sens Actuators B 103(1):339–343. doi: https://doi.org/10.1016/j.snb.2004.04.063
36. Zhang Q, Li C (2020) High temperature stable anatase phase titanium dioxide films synthesized by mist chemical vapor deposition. Nanomaterials. https://doi.org/10.3390/nano10050911
37. Abe M, Mori T, Osaka I, Sugimoto K, Takimiya K, Thermally (2015) Operationally, and environmentally stable organic thin-film transistors based on bis[1]benzothieno[2,3-d:2′,3′-d′]naphtho[2,3-b:6,7-b′]dithiophene derivatives: effective synthesis, electronic structures, and structure–property relationship. Chem Mater 27(14):5049–5057. https://doi.org/10.1021/acs.chemmater.5b01608

Publisher's note